THE JOURNAL OF PHYSICAL CHEMISTRY Letters

Letter

pubs.acs.org/JPCL

Electronic Structures of Formic Acid (HCOOH) and Formate ($HCOO^-$) in Aqueous Solutions

Matthew A. Brown,*[,†] Fernando Vila,[‡] Martin Sterrer,[§] Stephan Thürmer,[∥] Bernd Winter,[∥] Markus Ammann,[⊥] John J. Rehr,[‡] and Jeroen A. van Bokhoven[†,#]

[†]Institute for Chemical and Bioengineering, ETH Zürich, CH-8093 Zürich, Switzerland

[‡]Department of Physics, University of Washington, Seattle, Washington, 98195, United States

[§]Department of Chemical Physics, Fritz-Haber-Institute der Max-Planck-Gesellschaft, D-14195 Berlin, Germany

[∥]Helmholtz-Zentrum Berlin für Materialien und Energie and BESSY, D-12489 Berlin, Germany

[⊥]Laboratory for Radiochemistry and Environmental Chemistry, Paul Scherrer Institute, CH-5232 Villigen PSI, Switzerland

[#]Swiss Light Source, Paul Scherrer Institute, CH-5232 Villigen PSI, Switzerland

ABSTRACT: The electronic structures of formic acid (HCOOH) and formate ($HCOO^-$) have been determined in aqueous solutions over a pH range of 1.88−8.87 using a combination of X-ray photoelectron spectroscopy (XPS), partial electron-yield X-ray absorption spectroscopy (PEY XAS), and density functional theory (DFT). The carbon 1s XPS measurements reveal a binding energy shift of −1.3 eV for deprotonated $HCOO^-$ compared with neutral HCOOH. Such distinction between neutral HCOOH and deprotonated $HCOO^-$ cannot be made based solely on the respective carbon K-edge PEY XA spectra. Independent of pH, the C1s → π^* state excitations occur at 288.0 eV and may lead to the incorrect conclusion that the energy levels of the π^* state are the same for both species. The DFT calculations are consistent with the experimental observations and show a shift to higher energy for both the occupied C1s (lower binding energy) and unoccupied π^* orbitals of deprotonated $HCOO^-$ compared to neutral HCOOH in aqueous solutions.

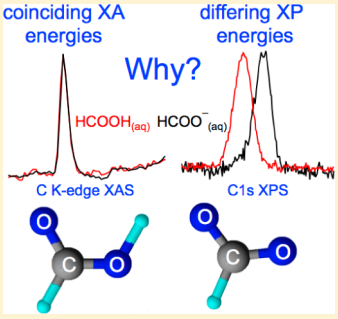

SECTION: Surfaces, Interfaces, Porous Materials, and Catalysis

Formic acid is an interesting molecule from a physical, chemical, and biological aspect. In addition to being the simplest of the carboxylic acids, which has made it a model for fundamental studies in both theory[1−5] and experiment,[6−10] formic acid has attracted renewed interest as a potential hydrogen storage material.[11−14]

In aqueous solution, formic acid establishes equilibrium with its conjugate base formate ($HCOO^-$). With a pK_a of 3.75 formic acid is normally categorized as being of intermediate strength and is mostly undissociated in a binary formic acid−water solution.[15] However, by varying the pH in solution, the equilibrium can be continuously varied and provides a means to generate one or the other, or both species, in aqueous solutions. At high pH, equilibrium favors deprotonated formate ($HCOO^-$), which is of particular significance in the field of catalysis, as a formate-metal complex is believed to be the stable intermediate adsorbed on the surface of the catalyst that precedes the production of H_2 and CO_2 during the dehydrogenation of HCOOH.[6,16]

Here we use a combination of in situ X-ray photoelectron spectroscopy (XPS) and in situ partial electron yield X-ray absorption spectroscopy (PEY XAS) from a liquid microjet to study the electronic structure of aqueous solutions of formic acid as a function of pH at the liquid−vapor interface.

XPS and XAS are complementary element-specific probes of local electronic structure with XPS[17] probing occupied- and XAS[18] probing unoccupied-states. In the case of (nonresonant) XPS,[17] the photon energy ($h\nu$) is taken to exceed the binding energy (BE) of the core electron. As a result of this ionization process, a photoelectron is ejected into vacuum with a kinetic energy that is measured and used to infer the corresponding BE. For light elements such as carbon, the core hole generated during the ionization process relaxes primarily (99%) by Auger decay. In the case of XAS,[18] a core electron is resonantly excited to an unoccupied state upon absorption of a photon, and by varying the incoming photon energy across the absorption edge, the energies of the respective empty states can be probed. The decay of the core hole (on carbon) that is created during excitation proceeds by Auger electron emission, which is assumed to be proportional to the XA spectrum. Hence, by integrating the Auger electron signal near the X-ray absorption (XA) edge as a function of incoming photon energy, the PEY XA spectrum is collected. It is important to note that XA energies contain no information on the absolute energies of the states involved in the absorption process. Only in conjunction with the respective core level binding energies or ionization onset, measured by XPS, can one assign an absolute energy to the unoccupied states.

Received: April 25, 2012
Accepted: June 18, 2012
Published: June 18, 2012

As we show here for the case of neutral HCOOH and deprotonated $HCOO^-$ in aqueous solutions, the carbon K-edge PEY XA spectra cannot be properly interpreted without a complementary C1s XPS experiment. Here we encounter the interesting situation that the XA spectra are essentially the same for the two species in aqueous solutions, and yet the levels involved are different on the absolute energy scale. Overlooking the absolute energy scale leads to a misinterpretation of the respective XA spectra. Also, while formic acid in aqueous solutions is surely not a singular case of coinciding XA energies, surprisingly, despite liquid microjets currently in operation at the Advanced Light Source,[19−22] BESSY,[23−26] MAX-lab,[27−29] and the Swiss Light Source,[30] there exist but a few studies to date that report simultaneous XPS and XAS results for a given solute in aqueous solution.[31−33]

This Letter is divided into three sections: First, we assign the absolute BE of the C1s core levels for both neutral HCOOH and deprotonated $HCOO^-$ in aqueous solutions using in situ XPS. Second, we present the respective carbon K-edge PEY XA spectra of both molecules in aqueous solutions. Third, DFT calculations are presented, providing detailed insight into the structural and electronic changes of formic acid in aqueous solutions as the protonation state is varied.

Figure 1 shows the C1s XP spectra of 1 M formic acid at pH 1.88, 3.75, and 8.87. The spectrum at pH 1.88 consists of a single peak centered at a BE of 294.8 eV (Figure 1a), which we assign to neutral HCOOH in aqueous solution. This BE is +1.0 eV above the one reported for the respective gas phase species, $HCOOH_{gas}$,[34] and in agreement with expected hydration-induced BE shifts.[31,35] As the pH is increased to the pK_a (3.75), a pronounced shoulder appears in the spectrum that requires a second component to properly fit (Figure 1b). This second component is centered at a BE of 293.5 eV, i.e., 1.3 eV below that of neutral HCOOH in aqueous solution, and can be assigned to deprotonated $HCOO^-$ in aqueous solution. Obviously, the −1.3 eV chemical shift in the C1s BE is sufficient to allow for the protonation state of formic acid to be identified in aqueous solutions. Despite equal bulk concentrations at pH 3.75 the C1s signal intensities of the two components differ considerably. The larger signal of the neutral HCOOH component would be qualitatively consistent with a considerable excess concentration of the neutral molecular form in the near surface region.[36] As the pH is further increased to 8.87, the equilibrium favors the conjugate base in solution, and the spectrum is dominated by deprotonated $HCOO^-$ (Figure 1c). The weak intensity component in this spectrum belongs to neutral HCOOH and suggests that either the surface excess at low bulk concentrations is significantly more enhanced than that observed at pH = pK_a (where the bulk concentration of neutral HCOOH is 0.5 M), or that the interface of this solution is more acidic than the bulk (thereby shifting the equilibrium toward neutral HCOOH). If the surface excess were assumed to be similar to that noted at pH = pK_a, where a ratio of ∼5:1 is recorded in the C 1s XP spectrum for $HCOOH:HCOO^-$, the concentration of neutral HCOOH at pH = 8.87 can be estimated (based on a ratio of ∼1:10) at below 2%.

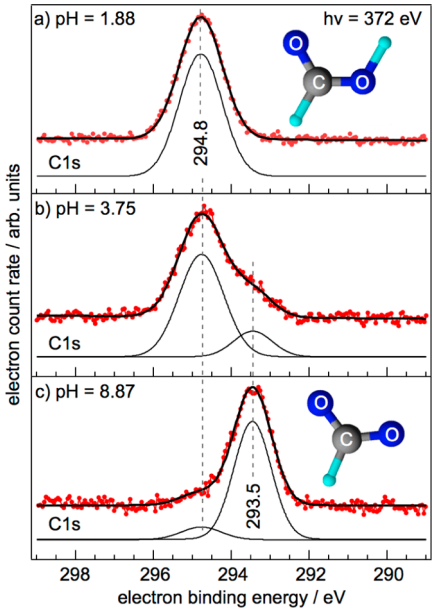

Figure 1. C1s photoelectron spectra of aqueous 1 M formic acid recorded at pH values of (a) 1.88, (b) 3.75 (corresponding to the bulk pK_a value), and (c) 8.87 with incident photon energy of 372 eV. The collected data following a Shirley background subtraction are shown as red squares, whereas the fits are shown in black. The BE scale is relative to the vacuum level.

Figure 2a shows the measured carbon K-edge PEY XA spectra for aqueous 1 M solutions of formic acid at pH 1.88 (black) and 8.87 (red). Unlike the XP spectra of Figure 1, the two XA spectra are essentially identical at the main (first peak) absorption, and there is no obvious indication that neutral HCOOH and deprotonated $HCOO^-$ in aqueous solutions could be easily identified based solely on the main absorption feature of these spectra. The main absorption at 288.0 eV is known to originate from the C1s → π* state excitation.[37,38]

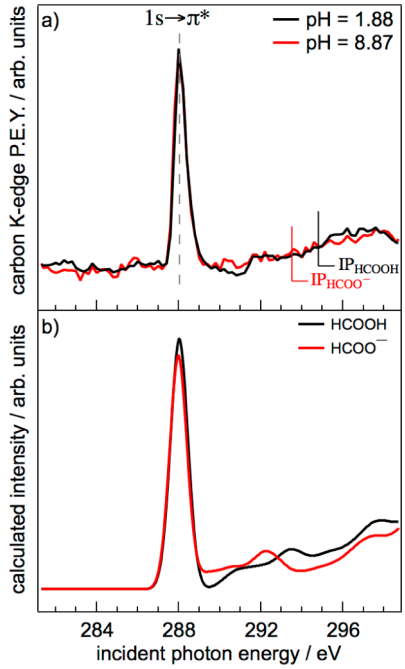

Figure 2. (a) Carbon K-edge PEY XA spectra of 1 M formic acid aqueous solution recorded at pH 1.88 (black) and 8.87 (red). Spectra were recorded in constant kinetic energy mode by monitoring the carbon Auger electron signal as the photon energy was swept across the absorption edge. (b) The corresponding calculated XA spectra as determined from TDDFT using both a dielectric solvation field and explicit solvation.

dx.doi.org/10.1021/jz300510r | J. Phys. Chem. Lett. 2012, 3, 1754−1759

The corresponding calculated XA spectra are shown in Figure 2b (and described below) and are in good agreement with the experiment when an energy resolution of 0.2 eV is taken into account. Small, subtle differences in the PEY XA spectra that might be used to identify the protonation state of formic acid in aqueous solutions do present themselves at photon energies above the main C1s → π^* state excitation and are also seen in the calculated spectra. However, the small signal intensity of the experimental spectra in this region does not allow for a safe assignment, and for the purpose of the current discussion, we focus our attention on the first absorption, i.e., main transition in the carbon K-edge PEY XA spectra.

What might mistakenly be concluded at this point based on the first absorption in the carbon K-edge PEY XA spectra is that the unoccupied π^* states of formic acid in aqueous solutions, regardless of protonation state, are identical in energy. This is obviously not the case, as dictated by our XPS measurements that show a pronounced dependence to the energy of the C1s core-level on the protonation state of formic acid in aqueous solutions. One thus has to be very careful when interpreting XA spectra (on their own) from solution, and one needs to understand the apparent discrepancy between the XPS and XAS results, and that requires state-of-the-art electronic structure calculations.

Density functional theory (DFT) calculations using a dielectric solvation field and explicit solvation for both neutral HCOOH and deprotonated $HCOO^-$ were performed to interpret the XPS and PEY XAS results. The optimized structures are shown in Figure 3a,b for neutral HCOOH and deprotonated $HCOO^-$, respectively. Formic acid was modeled as a monomer, as the dimer does not exist in dilute aqueous solution (1 molar).[39] Structural optimizations were performed at the B3LYP level and are summarized in Table 1. Both molecules were explicitly solvated by four water molecules.

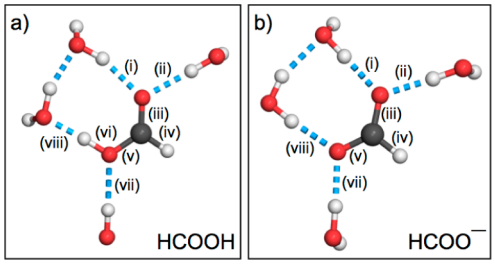

Figure 3. Optimized structures used for the simulations of solvated (a) neutral HCOOH and (b) deprotonated $HCOO^-$. Structural optimizations were performed at the B3LYP level and include a polarizable continuum model to account for dielectric solvation effects. Both neutral HCOOH and deprotonated $HCOO^-$ are explicitly solvated by four water molecules, and their hydrogen bonds are shown in blue. Roman numerals correspond to the structural parameters shown in Table 1.

The main differences between the optimized structures of neutral HCOOH and deprotonated $HCOO^-$ are as follows: There is a rearrangement of the hydrogen bonding network, with most of the bonds in deprotonated $HCOO^-$ getting shorter, and the C−O bonds in the formate ion become nearly symmetric and slightly shorter on average. The optimized bond lengths for both structures are summarized in Table 1.

Theoretical chemical BE shifts are most often approximated by the difference between the core state energies in the two chemical environments and usually are accurate to within 0.1 eV.[40,41] Our present calculations predict a chemical shift of 1.4 eV in the C1s orbital, in very good agreement with the observed value of 1.3 eV. A chemical shift of this magnitude is significant, in particular when we note that the spatial distribution of the C1s orbital remains well localized on the absorber and virtually unchanged after deprotonation. The electrostatic environment in and around the carbon atom, however, is significantly affected by the general redistribution of charge. To assess these changes on a quantitative level, we performed a natural atomic orbital analysis of the DFT wave functions[42] and find that the natural electron configuration of the C atom in neutral HCOOH is $1s^2\ 2s^{0.884}\ 2p^{2.370}$, whereas in deprotonated $HCOO^-$ the configuration is $1s^2\ 2s^{0.871}\ 2p^{2.417}$. Therefore, going from neutral HCOOH to deprotonated $HCOO^-$ in our solvated model results in a loss of 2s and a gain of 2p electrons on the carbon atom, with the latter dominating for an overall net gain of about 0.034*e*. These configurations are roughly what are expected for an atom with sp^2 hybridization. More interestingly, the small changes in electron occupation that give rise to the chemical BE shift can be assigned to the local rearrangement of the bonds that increases their π−over−σ character.

Table 1. Optimized Bond Lengths for the Structural Models of Neutral HCOOH and Deprotonated $HCOO^-$ Using a Dielectric Solvation Field and Explicit Solvation at the B3LYP Level

bond (Figure 3)	HCOOH/Å	$HCOO^-$/Å
i	2.839	2.732
ii	2.866	2.739
iii	1.226	1.265
iv	1.100	1.113
v	1.316	1.260
vi	1.023	
vii	2.964	2.736
viii	2.593	2.814

Given that chemical shift effects are usually quite local, we have used the above configurations to study the change in the C1s orbital energy in atomic simulations. Remarkably, isolated carbon atoms with the neutral HCOOH and deprotonated $HCOO^-$ configurations discussed above exhibit a chemical shift of 1.2 eV, nearly identical to the theoretical chemical shift of 1.4 eV predicted for the molecular systems. Moreover, this shift depends mostly on the total charge difference between the atoms and is nearly independent of the actual orbital occupations.

Unlike the core states, the unoccupied valence states involved in the XA excitations are more directly affected by the structural rearrangement upon deprotonation of formic acid. Our simulations predict that the prominent feature observed in the XA spectra arises from excitations to the π^* state,[37,38] which is shown in Figure 4 for both neutral HCOOH and deprotonated $HCOO^-$. As discussed above, the key structural rearrangement upon deprotonation of formic acid is the shortening of the C−O bonds. Since the π^* state has mainly antibonding character, particularly between the C and O atoms, the shortening of the C−O bonds results in a destabilization of the π^* state and an increase in its energy.

The net effect of increased electron density at the carbon atom and the destabilization of the π^* state in going from neutral HCOOH to deprotonated $HCOO^-$ can be seen in the simulated XA spectra shown in Figure 2b. The spectra of both

dx.doi.org/10.1021/jz300510r | J. Phys. Chem. Lett. 2012, 3, 1754−1759

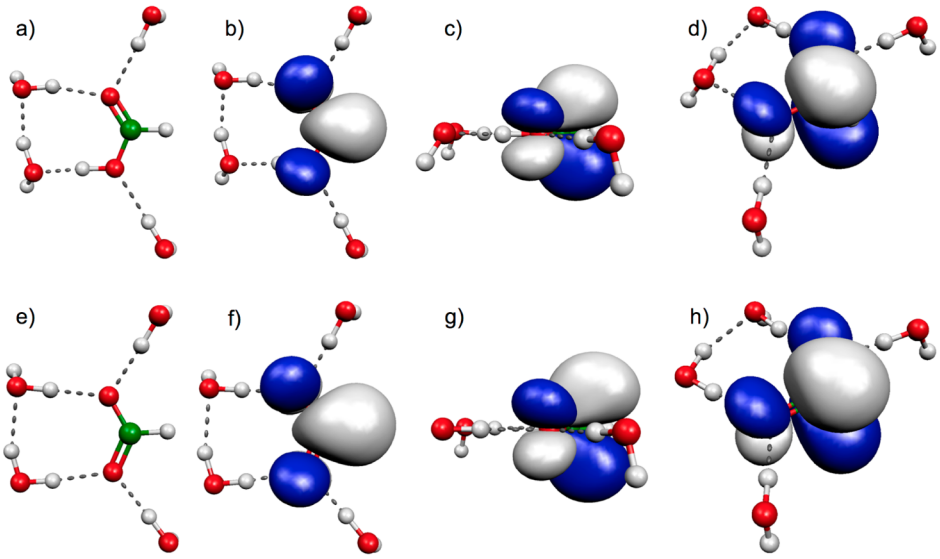

Figure 4. π^* states of neutral HCOOH (top) and deprotonated $HCOO^-$ (bottom). Views from the top (b,f), side (c,g), and perspective (d,h) are shown. The π^* state is extended over the whole molecule, but does not extend to the solvation shell. For clarity and to identify the position of the atoms, structures a and e are included with the π^* states removed.

molecules consist of a single intense C1s → π^* state excitation at 288.0 eV that renders the protonation state of formic acid in aqueous solutions indistinguishable using only the first absorption in the carbon K-edge spectra. The intensity of the K-edge XA spectra can be qualitatively understood by considering the dipole operator-mediated overlap between the core and excited state: Since the core has s symmetry and is highly localized around the absorber, the final state must have p symmetry and also have reasonable weight on the absorber. As shown in Figure 4, this is clearly the case for the out-of-plane π^* state. Other excitations of much less intensity appear at higher energies in the spectra. These less intense features starting at ∼291 eV correspond to excitations to in-plane states that have only partial p symmetry and are much less localized on the absorber, which is why they are difficult to observe in the experiment.

In situ XPS and PEY XAS measurements have been used to identify the protonation state of formic acid in aqueous solutions over a broad range of pH. The 1.3 eV chemical BE shift of the C1s orbital between neutral HCOOH and deprotonated $HCOO^-$ makes identifying the protonation state of formic acid in aqueous solutions using XPS trivial. By contrast, the similarity at the first excitation makes identifying the protonation state of formic acid in aqueous solutions using only carbon K-edge PEY XAS nontrivial. The chemical BE shift in the C1s orbital is well reproduced in DFT models only when a dielectric solvation field and explicit solvation are both included. The origin of the similarities in the carbon K-edge PEY XA spectra between neutral HCOOH and deprotonated $HCOO^-$ was shown to originate from an increase in energy of the π^* state of deprotonated $HCOO^-$ that perfectly offsets the increase in energy (decrease in BE) of the C1s orbital. The net effect is that the C1s → π^* excitations occur at 288.0 eV for formic acid in aqueous solutions, irrespective of protonation state. These findings appear to also be valid for the pH-dependent electronic structures of acetic acid in aqueous solutions (coinciding XA energies with differing XP energies),[43] which suggests the present conclusions may be general to carboxylic acids beyond formic and acetic acids.

The present Letter has demonstrated the benefit of combined electronic structure measurements using the complementary probes XPS and XAS. Taken together, XPS and XAS are capable of providing more detailed electronic structure information than the sum of the two techniques on their own and therefore, when experimentally possible, both should be performed.

■ EXPERIMENTAL METHODS

Our XPS and PEY XAS experiments were performed at the PGM-U41 beamline of BESSY using a 28 um liquid jet[44,45] operating at 279 K (measured immediately before expansion into the measurement chamber) and a flow rate of 0.65 mL/min. Three solutions of 1 M formic acid (Sigma-Aldrich) were prepared for analysis. The first solution was prepared at pH 1.88 by directly diluting the stock formic acid solution. A second solution was prepared at the room temperature pK_a value, pH 3.75, by the addition of concentrated NaOH (Sigma-Aldrich). A third solution was prepared at the equivalence point, pH 8.87, also by the addition of concentrated NaOH. Bulk pH values were measured at room temperature using a calibrated pH probe. It should be noted that the pK_a of formic acid exhibits only minor temperature dependence between 298 and 279 K, ∼1%,[46] and therefore is not expected to impact the present experiments, which were conducted at 279 K but prepared at 298 K.

XPS. C1s XP spectra were collected using a monochromatic incident photon energy of 372 eV, which results in an electron kinetic energy of ∼80 eV. The hemispherical electron energy analyzer was set to a constant pass energy of 10 eV. Reported binding energies are relative to the vacuum level and calibrated to the $1b_1$ orbital of liquid water at 11.16 eV.[47] The C1s spectral region was fit using pure Gaussian functions following a standard Shirley background subtraction.

PEY XAS. PEY XA spectra were collected in constant kinetic energy mode by monitoring the carbon Auger electron signal (∼260 eV KE) as the photon energy was swept in increments of 0.2 eV across the carbon K-absorption edge. The experiment is performed in the following manner: For each photon energy

dx.doi.org/10.1021/jz300510r | J. Phys. Chem. Lett. 2012, 3, 1754−1759

between 280 and 299 eV the hemispherical energy analyzer is scanned across an electron kinetic energy range of 200−300 eV at a pass energy of 100 eV and the resulting spectrum is integrated across the 100 eV energy window. The integration of each spectrum yields a single data point of the PEY XA spectrum. Background measurements (I_0) from a microjet of pure water were performed in an analogous manner to those of the formic acid solutions and used to normalize the PEY XA spectra to account for variations in the beamline flux at the sample position. It is generally agreed that the probe depth of an electron spectroscopy experiment at the liquid−vapor interface carried out at 80 eV (PES, above) and 260 eV (PEY XAS) varies by only 10% with the PES experiment being more surface sensitive.[48] Therefore the small contribution of neutral HCOOH in the PE spectrum at pH 8.87 is weighted to an even lesser extent in the PEY XAS measurements and not expected to affect the interpretation of the results.

COMPUTATIONAL METHODS

All simulations were performed using Gaussian 09.[49] Formic acid and formate were solvated with four explicit water molecules and optimized using the B3LYP exchange-correlation (XC) functional[50,51] and the aug-cc-pVDZ basis set,[52,53] resulting in the structures shown in Figure 3. In addition to the explicit solvent molecules, these optimizations were performed in the presence of a solvation reaction field using the water dielectric constant.[54] The solvation field is critical in bringing the C1s chemical shift into qualitative agreement with experiment since, in its absence, the resulting values were overestimated by about 5 eV. The explicit hydrogen-bonded water molecules play a less critical but nonetheless important role and bring the chemical shift into quantitative agreement with the experiment. The convergence of the chemical shift with respect to explicit solvation was verified by removing one of the water molecules (bond "ii" in Figure 3). This resulted in a change in chemical shift of only 0.1 eV. The chemical shift was computed by taking the difference of the Kohn−Sham energies for the corresponding C1s molecular orbitals.

The simulated XA spectra were computed using the TDDFT approach,[55,56] with the same XC functional and basis set as for the optimizations, with broadening included to match that observed in experiment. To ensure that only excitations from the core were included, all other occupied orbitals were kept frozen. It should be noted that although more sophisticated methods exist for computing XA spectra (e.g., those implemented in StoBe[57] or FEFF[58]), they lack the solvation reaction field required to obtain quantitative results in the specific application presented herein.

AUTHOR INFORMATION

Corresponding Author

*E-mail: matthew.brown@chem.ethz.ch.

Notes

The authors declare no competing financial interest.

ACKNOWLEDGMENTS

M.A.B. acknowledges financial support from the ETH Postdoctoral Fellowship Program. This work was supported in part by DOE Grant DE-FG03-97ER45623 (F.D.V. and J.J.R.) and with computer support from NERSC. B.W. acknowledges the Deutsche Forschungsgemeinschaft (Project WI 1327/3-1) for support.

REFERENCES

(1) Bakó, I.; Hutter, J.; Palinkas, G. Car−Parrinello Molecular Dynamics Simulation of Liquid Formic Acid. *J. Phys. Chem. A* **2006**, *110*, 2188−2194.

(2) Lee, J.-G.; Asciutto, E.; Babin, V.; Sagui, C.; Darden, T.; Roland, C. Deprotonation of Solvated Formic Acid: Car−Parrinello and Metadynamics Simulations. *J. Phys. Chem. B* **2006**, *110*, 2325−2331.

(3) Zhou, Z. Y.; Shi, Y.; Zhou, X. M. Theoretical Studies on the Hydrogen Bonding Interaction of Complexes of Formic Acid with Water. *J. Phys. Chem. A* **2004**, *108*, 813−822.

(4) Leung, K.; Rempe, S. B. Ab Initio Molecular Dynamics Study of the Aqueous Formate Ion. *J. Am. Chem. Soc.* **2003**, *126*, 344−351.

(5) Lintuluoto, M.; Nakatsuji, H.; Hada, M.; Kanai, H. Theoretical Study of the Decomposition of HCOOH on an MgO(100) Surface. *Surf. Sci.* **1999**, *429*, 133−142.

(6) Mars, P.; Scholten, J. J. F.; Zwietering, P. The Catalytic Decomposition of Formic Acid. *Adv. Catal.* **1963**, *14*, 35−113.

(7) Birer, O.; Havenith, M. High Resolution Infrared Spectroscopy of the Formic Acid Dimer. *Annu. Rev. Phys. Chem.* **2009**, *60*, 263−275.

(8) Columbia, M. R.; Thiel, P. A. The Interaction of Formic-Acid with Transition-Metal Surfaces, Studied in Ultrahigh-Vacuum. *J. Electroanal. Chem.* **1994**, *369*, 1−14.

(9) Śmiechowski, M.; Gojlo, E.; Stangret, J. Hydration of Simple Carboxylic Acids from Infrared Spectra of HDO and Theoretical Calculations. *J. Phys. Chem. B* **2011**, *115*, 4834−4842.

(10) Johnson, C. M.; Tyrode, E.; Kumpulainen, A.; Leygraf, C. Vibrational Sum Frequency Spectroscopy Study of the Liquid/Vapor Interface of Formic Acid/Water Solutions. *J. Phys. Chem. C* **2009**, *113*, 13209−13218.

(11) Makowski, P.; Thomas, A.; Kuhn, P.; Goettmann, F. Organic Materials for Hydrogen Storage Applications: From Physisorption on Organic Solids to Chemisorption in Organic Molecules. *Energ. Environ. Sci.* **2009**, *2*, 480−490.

(12) Fukuzumi, S. Bioinspired Energy Conversion Systems for Hydrogen Production and Storage. *Eur. J. Inorg. Chem.* **2008**, *9*, 1351−1362.

(13) Enthaler, S.; von Langermann, J.; Schmidt, T. Carbon Dioxide and Formic Acid − The Couple for Environmental-Friendly Hydrogen Storage? *Energy and Environmental Science* **2010**, *3*, 1207−1217.

(14) Jiang, H.-L.; Singh, S. K.; Yan, J.-M.; Zhang, X.-B.; Xu, Q. Liquid-Phase Chemical Hydrogen Storage: Catalytic Hydrogen Generation under Ambient Conditions. *ChemSusChem* **2010**, *3*, 541−549.

(15) Lide, D. R. *CRC Handbook of Chemistry and Physics*; CRC Press: Boca Raton, FL, 2010.

(16) Tedsree, K.; Li, T.; Jones, S.; Chan, C. W. A.; Yu, K. M. K.; Bagot, P. A. J.; Marquis, E. A.; Smith, G. D. W.; Tsang, S. C. E. Hydrogen Production from Formic Acid Decomposition at Room Temperature using a Ag-Pd Core-Shell Nanocatalyst. *Nat. Nanotechnol.* **2011**, *6*, 302−307.

(17) Hüfner, S. *Photoelectron Spectroscopy: Principles and Applications*; Springer-Verlag: Berlin, 1995.

(18) Koningsberger, D. C.; Prins, R. *X-Ray Absorption*; John Wiley and Sons: New York, 1988.

(19) Brown, M. A.; D'Auria, R.; Kuo, I.-F. W.; Krisch, M. J.; Starr, D. E.; Bluhm, H.; Tobias, D. J.; Hemminger, J. C. Ion Spartial Distributions at the Liquid−Vapor Interface of Aqueous Potassium Fluoride Solutions. *Phys. Chem. Chem. Phys.* **2008**, *10*, 4778−4784.

(20) Wilson, K. R.; Cavalleri, M.; Rude, B. S.; Schaller, R. D.; Catalano, T.; Nilsson, A.; Saykally, R. J.; Pettersson, L. G. M. X-ray Absorption Spectroscopy of Liquid Methanol Microjets: Bulk Electronic Structure and Hydrogen Bonding Network. *J. Phys. Chem. B* **2005**, *109*, 10194−10203.

(21) Messer, B. M.; Cappa, C. D.; Smith, J. D.; Wilson, K. R.; Gilles, M. K.; Cohen, R. C.; Saykally, R. J. pH Dependence of the Electronic Structure of Glycine. *J. Phys. Chem. B* **2005**, *109*, 5375−5382.

(22) Duffin, A. M.; England, A. H.; Schwartz, C. P.; Uejio, J. S.; Sallinger, G. C.; Shih, O.; Prendergast, D.; Saykally, R. J. Electronic

Structure of Aqueous Borohydride: A Potential Hydrogen Storage Medium. *Phys. Chem. Chem. Phys.* **2011**, *13*, 17077−17083.
(23) Brown, M. A.; Seidel, R.; Thürmer, S.; Faubel, M.; Hemminger, J. C.; van Bokhoven, J. A.; Winter, B.; Sterrer, M. Electronic Structure of Sub-10 nm Colloidal Silica Nanoparticles Measured by In Situ Photoelectron Spectroscopy at the Aqueous-Solid Interface. *Phys. Chem. Chem. Phys.* **2011**, *13*, 12720−12723.
(24) Brown, M. A.; Winter, B.; Faubel, M.; Hemminger, J. C. Spatial Distribution of Nitrate and Nitrite Anions at the Liquid/Vapor Interface of Aqueous Solutions. *J. Am. Chem. Soc.* **2009**, *131*, 8354−8355.
(25) Nolting, D.; Aziz, E. F.; Ottosson, N.; Faubel, M.; Hertel, I. V.; Winter, B. pH-Induced Protonation of Lysine in Aqueous Solution Causes Chemical Shifts in X-ray Photoelectron Spectroscopy. *J. Am. Chem. Soc.* **2007**, *129*, 14068−14073.
(26) Aziz, E. F.; Ottosson, N.; Eisebitt, S.; Eberhardt, W.; Jagoda-Cwiklik, B.; Vácha, R.; Jungwirth, P.; Winter, B. Cation-Specific Interactions with Carboxylate in Amino Acid and Acetate Aqueous Solutions: X-ray Absorption and ab Initio Calculations. *J. Phys. Chem. B* **2008**, *112*, 12567−12570.
(27) Ottosson, N.; Børve, K. J.; Spångberg, D.; Bergersen, H.; Sæthre, L. J.; Faubel, M.; Pokapanich, W.; Öhrwall, G.; Björneholm, O.; Winter, B. On the Origins of Core-Electron Chemical Shifts of Small Biomolecules in Aqueous Solution: Insights from Photoemission and ab Initio Calculations of $Glycine_{aq}$. *J. Am. Chem. Soc.* **2011**, *133*, 3120−3130.
(28) Bergersen, H.; Marinho, R. R. T.; Pokapanich, W.; Lindblad, A.; Björneholm, O.; Sæthre, L. J.; Öhrwall, G. A Photoelectron Spectroscopic Study of Aqueous Tetrabutylammonium Iodide. *J. Phys.: Condens. Matter* **2007**, *19*, 326101.
(29) Pokapanich, W.; Bergersen, H.; Bradeanu, I. L.; Marinho, R. R. T.; Lindblad, A.; Legendre, S.; Rosso, A.; Svensson, S.; Björneholm, O.; Tchaplyguine, M.; et al. Auger Electron Spctroscopy as a Probe of the Solution of Aqueous Ions. *J. Am. Chem. Soc.* **2009**, *131*, 7264−7271.
(30) Brown, M. A.; Huthwelker, T.; Beloqui Redondo, A.; Janousch, M.; Faubel, M.; Arrell, C. A.; Scarongella, M.; Chergui, M.; van Bokhoven, J. A. Changes in Silanol Protonation State Measured In Situ at the Silica-Aqueous Interface. *J. Phys. Chem. Letters* **2012**, *3*, 231−235.
(31) Ottosson, N.; Aziz, E. F.; Bergersen, H.; Pokapanich, W.; Öhrwell, G.; Svensson, S.; Eberhardt, W.; Björneholm, O. Electronic Rearrangement upon the Hydrolyzation of Aqueous Formaldehyde Studied by Core-Electron Spectroscopies. *J. Phys. Chem. B* **2008**, *112*, 16642−16646.
(32) Thürmer, S.; Seidel, R.; Eberhardt, W.; Bradforth, S. E.; Winter, B. Ultrafast Hybridization Screening in Fe^{3+} Aqueous Solution. *J. Am. Chem. Soc.* **2011**, *133*, 12528−12535.
(33) Seidel, R.; Ghadimi, S.; Lange, K. M.; Bonhommeau, S.; Soldatov, M. A.; Golnak, R.; Kothe, A.; Könnecke, R.; Soldatov, A.; Thürmer, S.; et al. Origin of Dark-Channel X-ray Fluorescence from Transition-Metal Ions in Water. *J. Am. Chem. Soc.* **2012**, *134*, 1600−1605.
(34) Smith, S. R.; Thomas, T. D. Acidities and Basicities of Carboxylic Acids. Correlations Between Core-Ionization Energies, Proton Affinities, and Gas-Phase Acidities. *J. Am. Chem. Soc.* **1978**, *100*, 5459−5466.
(35) Winter, B. Liquid Microjet for Photoelectron Spectroscopy. *Nucl. Instrum. Methods Phys. Res., Sect. A* **2009**, *601*, 139−150.
(36) Ottosson, N.; Wernersson, E.; Söderström, J.; Pokapanich, W.; Kaufmann, S.; Svensson, S.; Persson, I.; Öhrwall, G.; Björneholm, O. The Protonation State of Small Carboxylic Acids at the Water Surface from Photoelectron Spectroscopy. *Phys. Chem. Chem. Phys.* **2011**, *13*, 12261−12267.
(37) Ishii, I.; Hitchcock, A. P. A Quantitative Experimental Study of the Core Excited Electronic States of Formamide, Formic Acid, and Methyl Fluoride. *J. Chem. Phys.* **1987**, *2*, 830−839.
(38) Outka, D. A.; Stöhr, J.; Madix, R. J.; Rotermund, H. H.; Hermsmeier, B.; Solomon, J. NEXAFS Studies of Complex Alcohols and Carboxylic Acids on the Si(111)(7 × 7) Surface. *Surf. Sci.* **1978**, *185*, 53−74.
(39) Colominas, C.; Teixidó, J.; Cemelí, J.; Luque, F. J.; Orozco, M. Dimerization of Carboxylic Acids: Reliability of Theoretical Calculations and the Effect of Solvent. *J. Phys. Chem. B* **1998**, *102*, 2269−2276.
(40) Vila, F. D.; Jach, T.; Elam, W. T.; Rehr, J. J.; Denlinger, J. D. X-ray Emission Spectroscopy of Nitrogen Rich Compounds. *J. Phys. Chem. A* **2011**, *115*, 3243−3250.
(41) Söderström, J.; Mårtensson, N.; Travnikova, O.; Patanen, M.; Miron, C.; Sæthre, L.; Børve, K.; Rehr, J. J.; Kas, J. J.; Vila, F. D.; et al. Non-Stoichiometric Intensities in Core Photoelectron Spectroscopy. *Phys. Rev. Lett.* **2012**, *108*, 193005.
(42) Weinhold, F.; Carpenter, J. E. *The Structure of Small Molecules and Ions*; Naaman, R., Vager, Z., Eds.; Plenum: New York, 1988; pp 227−236, and references therein.
(43) Krepelova, A.; Bartels-Rausch, T.; Brown, M. A.; Bluhm, H.; Ammann, M. The Adsorption of Acetic Acid on Ice Studied by XPS and NEXAFS. To be submitted for publication, 2012.
(44) Brown, M. A.; Faubel, M.; Winter, B. X-ray Photo- and Resonant Auger-Electron Spectroscopy Studies of Liquid Water and Aqueous Solutions. *Annu. Rep. Prog. Chem., Sect. C: Phys. Chem.* **2008**, *105*, 174−212.
(45) Winter, B.; Faubel, M. Photoemission from Liquid Aqueous Solutions. *Chem. Rev.* **2006**, *106*, 1176−1211.
(46) Kim, M. H.; Kim, C. S.; Lee, H. W.; Kim, K. Temperature Dependence of Dissociation Constants for Formic Acid and 2,6-Dinitrophenol in Aqueous Solutions up to 175°C. *J. Chem. Soc., Faraday Trans.* **1996**, *92*, 4951−4956.
(47) Winter, B.; Weber, R.; Widdra, W.; Dittmar, M.; Faubel, M.; Hertel, I. V. Full Valence Band Photoemission from Liquid Water using EUV Synchrotron Radiation. *J. Phys. Chem. B* **2004**, *108*, 2625−2632.
(48) Ottosson, N.; Faubel, M.; Bradforth, S. E.; Jungwirth, P.; Winter, B. Photoelectron Spectroscopy of Liquid Water and Aqueous Solution: Electron Effective Attenuation Lengths and Emission-Angle Anisotropy. *J. Electron Spectrosc.* **2010**, *177*, 60−70.
(49) Frisch, M. J.; Trucks, G. W.; Schlegel, H. B.; Scuseria, G. E.; Robb, M. A.; Cheeseman, J. R.; Scalmani, G.; Barone, V.; Mennucci, B.; Petersson, G. A.; et al. *Gaussian 09*, revision B.01; Gaussian, Inc.: Wallingford, CT, 2010.
(50) Becke, A. D. Density-Functional Thermochemistry. III. The Role of Exact Exchange. *J. Chem. Phys.* **1993**, *98*, 5648−5652.
(51) Lee, C.; Yang, W.; Parr, R. G. Development of the Colle−Salvetti Correlation-Energy Formula into a Functional of the Electron Density. *Phys. Rev. B* **1988**, *37*, 785−789.
(52) Kendall, R. A.; Dunning, T. H., Jr.; Harrison, R. J. Electron Affinities of the First-Row Atoms Revisited. Systematic Basis Sets and Wave Functions. *J. Chem. Phys.* **1992**, *96*, 6796−6806.
(53) Woon, D. E.; Dunning, T. H., Jr. Gaussian-Basis Sets for Use in Correlated Molecular Calculations. 3. The Atoms Aluminum through Argon. *J. Chem. Phys.* **1993**, *98*, 1358−1371.
(54) Tomasi, J.; Mennucci, B.; Cammi, R. Quantum Mechanical Continuum Solvation Models. *Chem. Rev.* **2005**, *105*, 2999−3093.
(55) Bauernschmitt, R.; Ahlrichs, R. Treatment of Electronic Excitations within the Adiabatic Approximation of Time Dependent Density Functional Theory. *Chem. Phys. Lett.* **1996**, *256*, 454−464.
(56) Casida, M. E.; Jamorski, C.; Casida, K. C.; Salahub, D. R. Molecular Excitation Energies to High-Lying Bound States from Time-Dependent Density-Functional Response Theory: Characterization and Correction of the Time-Dependent Local Density Approximation Ionization Threshold. *J. Chem. Phys.* **1998**, *108*, 4439−4449.
(57) Triguero, L.; Pettersson, L.; Agren, H. J. Calculations of X-ray Emission Spectra of Molecules and Surface Adsorbates by Means of Density Functional Theory. *Phys. Chem. A* **1998**, *102*, 10599−10607.
(58) Rehr, J. J.; Kas, J. J.; Prange, M. P.; Sorini, A. P.; Takimoto, Y.; Vila, F. Ab Initio Theory and Calculations of X-Ray Spectra. *C. R. Phys.* **2008**, DOI: 10.1016/j.crhy.2008.08.004.